

Split vortices in optically coupled Bose-Einstein condensates

Juan J. García-Ripoll and Víctor M. Pérez-García

Departamento de Matemáticas, Escuela Técnica Superior de Ingenieros Industriales, Universidad de Castilla-La Mancha, 13071 Ciudad Real, Spain

Fernando Sols

Departamento de Física Teórica de la Materia Condensada e Instituto "Nicolás Cabrera," Universidad Autónoma de Madrid, Cantoblanco, Spain

(Received 22 September 2001; published 13 August 2002)

We study a rotating two-component Bose-Einstein condensate in which an optically induced Josephson coupling allows for population transfer between the two species. In a regime where separation of species is favored, the ground state of the rotating system displays domain walls with velocity fields normal to them. Such a configuration looks like a vortex split into two halves, with atoms circulating around the vortex and changing their internal state as they cross the domain wall.

DOI: 10.1103/PhysRevA.66.021602

PACS number(s): 03.75.Fi, 67.57.Fg, 67.90.+z

Vortex formation is generally viewed as an unequivocal signature of superfluid motion in atomic Bose-Einstein condensates. Both in one- and two-component systems, a number of vortexlike structures have been created and observed [1,2] that confirm theoretical predictions [3–5]. The Josephson effect between two weakly coupled condensates is another paradigm of superfluid transport that so far has received less attention [6–8]. In this paper, we present a combined study of these two fundamental properties of superfluid systems: vortex and Josephson dynamics. We study the ground-state properties of a rotating double condensate system in which the combined role of vortex formation and optical coupling between two different hyperfine states gives rise to a rich physical behavior.

A crucial consequence of the internal Josephson coupling is the generation of an *effective attraction* between both atomic species due to the energy that atoms gain by choosing a symmetric mixture of the coupled internal states. Therefore, the most interesting physics is reached by combining this coupling with setups that otherwise favor species separation, such as a particular combination of atomic scattering lengths [9,10] or a separation of the respective confining potentials [11]. In these types of setups we find that the effective attraction due to the optical coupling causes an increase in the thickness of the domain wall where the two components physically overlap. More important is the fact that, if we add rotation to a Josephson coupled condensate with separate domains, atoms can use the domain wall to mutate their internal state and shift between components in a continuous way. Combining this persistent current in the inner space with a persistent current in real space, the double condensate may now easily create a vortex core for each component in the region where that component has a low density. Even for otherwise small values of the Josephson coupling, these *split vortices* support a net mass flow comparable to that of conventional vortices. The formation of these novel structures is less costly in terms of angular speed because the vortex of a given component is formed not within its own domain but in the opposite one, where its superfluid density is low and the cost in kinetic energy is therefore small.

To study this type of vortex structure, we analyze first a rotating two-component condensate without optical coupling (i.e., with impenetrable domain walls) and show that its behavior is essentially that of a one-component system with a displaced axis of rotation. Then we show that vortex formation is strongly inhibited because of the ability of the system to gain angular momentum by merely distancing itself from the rotation axis. The picture changes qualitatively when a Raman coupling is introduced to permit coherent hopping between the two internal states. Because the flow of particles in a given state is no longer a conserved quantity, the circulation lines of a component can cross the domain wall with a concomitant decrease in their supporting superfluid density. This results in a global structure of two asymmetrical vortices where matter is efficiently transported both in real space and within the hyperfine doublet.

I. THE MODEL

In this paper we focus on double condensate systems such as those made of Rb at JILA [1], but this time in rotating traps and with a permanent optical coupling between the species. In the rotating frame of Ref. [5], the Gross-Pitaevskii equations for the condensate wave functions read

$$i\hbar\partial_\tau\Psi_1 = \left[H_1 + \sum_j U_{1j}|\Psi_j|^2 \right] \Psi_1 - \frac{1}{2}\hbar\Omega_R\Psi_2, \quad (1a)$$

$$i\hbar\partial_\tau\Psi_2 = \left[H_2 + \sum_j U_{2j}|\Psi_j|^2 \right] \Psi_2 - \frac{1}{2}\hbar\Omega_R\Psi_1. \quad (1b)$$

Here H_j correspond to the noninteracting Hamiltonians $H_{1,2} = -(\hbar^2/2m)\Delta + V(\mathbf{r}-\mathbf{r}_{1,2}) - \hbar\Omega L_z + \hbar\bar{\delta}_{1,2}$, where $V(\mathbf{r}) = \frac{1}{2}m\omega^2r^2$ is the trapping potential, \mathbf{r}_j is the center of the trap for component j , and Ω is the angular speed. The mutual interactions $U_{ij} = 4\pi\hbar^2 a_{ij}/m$ are proportional to the s -wave scattering lengths a_{ij} . The last term in each equation models an optical coupling between species. This is a Josephson-type coupling that allows atoms to change their internal state. Since we focus on stationary configurations, the normalization of each wave function is fixed, $N_i = \int |\Psi_i(\mathbf{r})|^2 d\mathbf{r}$. Fi-

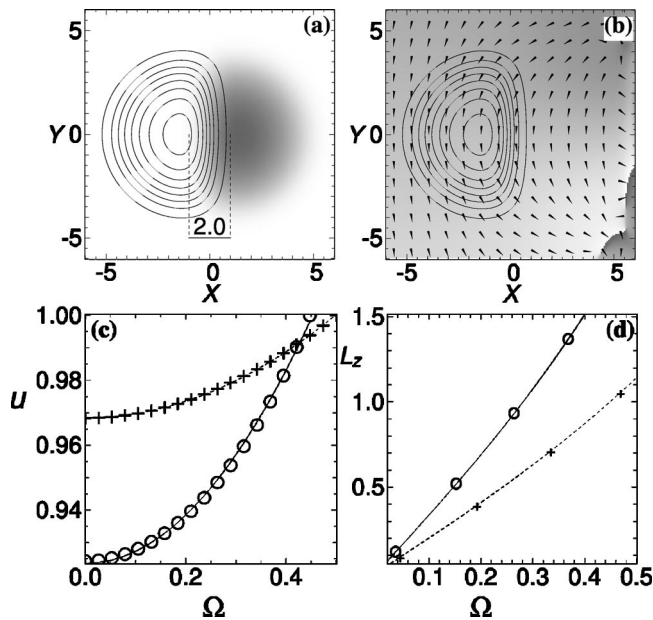


FIG. 1. (a) Density profiles in scenario A for $\Omega=0$. We show a gray-scale plot of $|\psi_1|^2$ (dark) and a contour plot of $|\psi_2|^2$ (solid lines). The trap separation is indicated with dashed lines. (b) Type A condensates for $\Omega=0.135$. Gray-scale plot for the phase ($\theta = \arg \psi_1$), arrows for the direction of the velocity field ($\mathbf{v} = \nabla \theta$), and contour lines for $|\psi_1|^2$. (c) Separation of the atomic clouds and (d) angular momentum as a function of the angular speed for scenarios A (circles, solid line) and B (crosses, dashed line). All magnitudes have been adimensionalized.

nally, $\hbar \bar{\delta}_i$ is a tunable energy splitting in the hyperfine space, which controls the population of each component.

In this paper, we restrict our attention to axially symmetric two-dimensional configurations which may describe pancake-type traps [12]. In such traps the nonlinear parameter is affected by a corrective factor [5] and N_1 and N_2 are interpreted as the effective number of particles. To facilitate the analysis, we introduce dimensionless variables $\mathbf{x} = \mathbf{r}/a_0$ and $t = \tau/T$. With this change and $\psi_j(\mathbf{x}, t) = N_j^{-1/2} \Psi_j(\mathbf{r}, \tau)$, we write the equations for stationary states

$$\mu_1 \psi_1 = \left[\mathcal{H}_1 + \sum_j g_{1j} |\psi_j|^2 \right] \psi_1 - \lambda \psi_2, \quad (2a)$$

$$\mu_2 \psi_2 = \left[\mathcal{H}_2 + \sum_j g_{2j} |\psi_j|^2 \right] \psi_2 - \lambda \psi_1, \quad (2b)$$

with rescaled Hamiltonians ($k=1,2$)

$$\mathcal{H}_k = \frac{1}{2} [-\Delta + (x - x_k)^2 + y^2] + i\Omega(x\partial_y - y\partial_x). \quad (3)$$

In Eq. (2), the splittings $\bar{\delta}_i$ are included in the chemical potentials. The parameter $\lambda = 2\Omega_R/\omega$ measures the intensity of the optical coupling. Although it is widely tunable, in our work it will be spatially uniform and at most of order unity. We have solved numerically Eq. (2), looking for the solu-

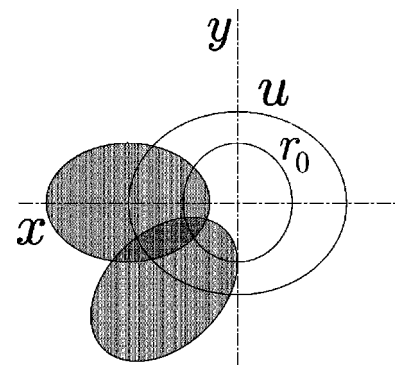


FIG. 2. Scheme of an off-axis rotating trap. Both the center of the trap and the trap itself rotate with angular speed Ω .

tions that have lower energy, the so-called ground states. Each of such solutions represents a stable, experimentally realizable configuration.

We will consider two different scenarios in which the double condensate exhibits domain walls, and which give qualitatively similar results. The first case, which we call “setup B,” corresponds to a situation in which $g_{11} = g_{22} = N$, $g_{12} = 2N$, with a choice of $N=38$. In this case the inequality $g_{12}^2 > g_{11}g_{22}$ is satisfied and the domains form spontaneously [10] with no need for trap separation nor splitting, i.e., $x_{1,2}=0$, $\mu_1 = \mu_2$.

The second and most important scenario, which we call “setup A,” corresponds to the case of ^{87}Rb [1] with parameter values $\begin{pmatrix} g_{11} & g_{12} \\ g_{21} & g_{22} \end{pmatrix} = \begin{pmatrix} 1 & 0.94 \\ 0.94 & 0.97 \end{pmatrix} \alpha N$ (i.e., $N_1 = N_2 = N$), and a typical effective value of $N=100$. This type of condensate has been studied in many previous experimental and theoretical works. For ^{87}Rb , the inequality mentioned above is close to saturation [10] and a separation $x_1 = -x_2 = 1$ ensures the formation of two different domains. The external splitting takes small values, $\mu_1 - \mu_2 \leq 0.01$, and it does not influence the results.

II. ROTATION WITHOUT JOSEPHSON COUPLING

Here we consider the case $\lambda = 0$. The existence of domain walls implies that the motion of species is spatially constrained. Therefore, if we impose some angular speed to the traps containing the condensates, each cloud tends to slip tangentially to the domain wall. The density distribution is similar to the case without rotation, but now, due to the centrifugal force, the species separate a little and gain linear speed. Together with the deformation of the clouds, this mechanism permits acquiring a large amount of angular momentum without generating vortices [Fig. 1(d)], which only form at very high Ω [>0.4 as Fig. 4(a) shows].

In Fig. 1(a), we show the ground state of the rotating double condensate system for $\lambda = 0$, showing a structure of domain walls that persists in the presence of rotation and prevents the formation of vortices, as revealed by the phase and circulation patterns of Fig. 1(b). From Fig. 1(c), it is evident that both the mutual repulsion and the rotation of the trap increase the separation among species. The flow pattern presents a curvature which is too small [Fig. 1(b)], and the

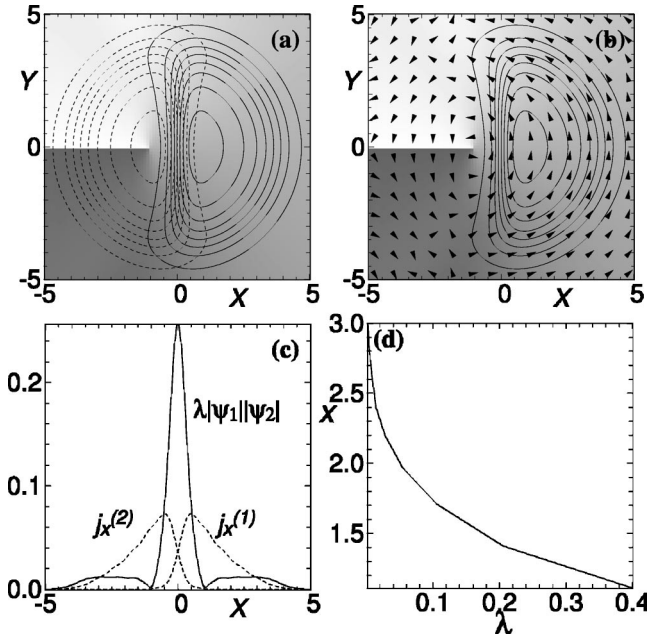


FIG. 3. Rotating two-component condensate with coupling $\lambda = 0.1$, scenario *B* with $N = 100$ and angular speed $\Omega = 0.2$. (a) Contour lines for the moduli of the wave functions $|\psi_1|$ (solid line) and $|\psi_2|$ (dashed line). (b) Contour levels for $|\psi_1|$, phase ($\theta = \arg \psi_1$, gray scale), and velocity field ($\mathbf{v}_1 = \nabla \arg \psi_1$, triangles). (c) Condensate fluxes $j_x^{(i)} = |\psi_i|^2 v_x^{(i)}$, together with intensity of the optical coupling, $\lambda |\psi_1| |\psi_2|$, along the line $y = -0.097$. (d) Position of the vortex for a type *B* condensate with $\Omega = 0.28$, as a function of the coupling. All units have been adimensionalized.

gain of angular momentum [Fig. 1(d)] is due instead to the displacement of the condensate away from the origin.

To get a deeper understanding of this configuration, it is useful to study the off-axis rotation of a single component condensate. It experiences a potential $V(\mathbf{x}, t) = \frac{1}{2} [\mathbf{x} - \mathbf{r}_0(t)] A(t) [\mathbf{x} - \mathbf{r}_0(t)]$ with $A(t)$ and $\mathbf{r}_0(t)$ rotating at speed Ω around a displaced axis, as depicted in Fig. 2. Thanks to a particular symmetry of the problem [13], the wave function for an off-axis rotating condensate can be written as a solution of the centered problem displaced a variable amount,

$$\psi_{\text{off}}(\mathbf{x}, t) = \phi_{\text{centered}}(\mathbf{x} - \mathbf{u}, t) e^{i m \mathbf{u} \cdot \mathbf{x} / \hbar + f(t)}. \quad (4)$$

This tells us that the behavior of a condensate in an off-axis rotating trap is qualitatively similar to that of a condensate in a centered trap: Vortices nucleate at similar angular speeds and they all appear inside the condensed cloud. The difference is that now the condensate has an additional source of angular momentum due to its displacement with respect to the origin, $L_z \propto \Omega |u|^2 \propto \Omega (1 - \Omega^2 / \omega^2)^{-2} r_0^2$.

These arguments, which are rigorous for the single condensate system, may be extended to the two-component condensate case when the overlap between clouds is small, meaning that vortices should appear in the center of the corresponding clouds even when each of the components is displaced from the axis of rotation.

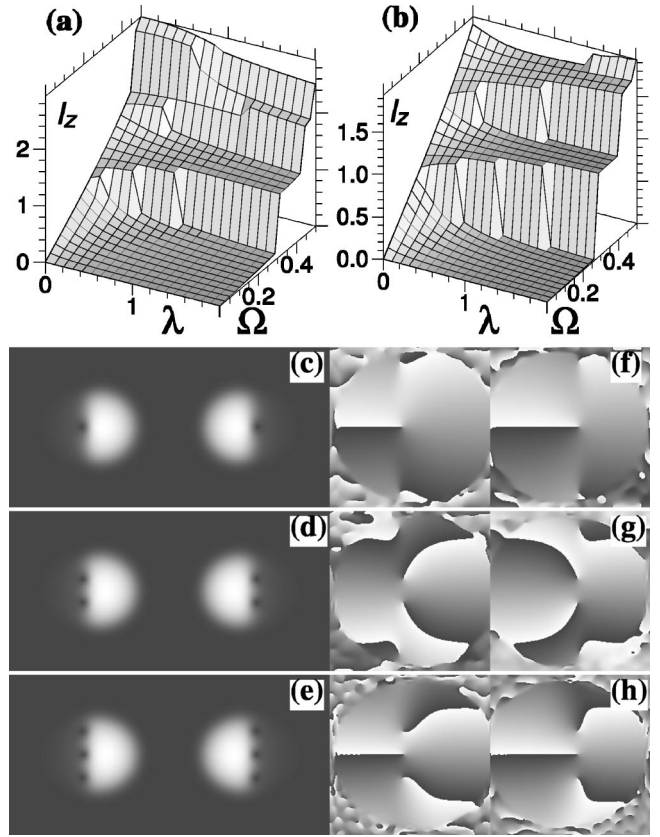


FIG. 4. (a), (b) Angular momentum per particle, l_z , versus Ω and λ , for type *A* and *B* condensates, respectively. (c)–(e) Density plots and (f)–(h) phase plots of states of a type *A* rotating condensate: $\lambda = 0.315$, $\Omega = 0.316$ (c), (f), $\Omega = 0.447$ (d), (g), and $\Omega = 0.474$ (e), (h). In (c)–(h) we plot both species separately (although they overlap). All magnitudes are dimensionless.

III. ROLE OF JOSEPHSON COUPLING

In order to explain the role of Josephson coupling, let us first consider situation *A*. It is easy to show that the Josephson terms favor energetically the mixing of both species. In the limit of strong coupling, they coexist in space even when their traps are separated. This is most intuitively appreciated by inspecting the energy functional associated to Eq. (2),

$$E[\psi_1, \psi_2] = \int [\bar{\psi}_1 \mathcal{H}_1 \psi_1 + \bar{\psi}_2 \mathcal{H}_2 \psi_2] + \int \left[\sum_{i,j=1,2} g_{ij} |\psi_j|^2 |\psi_i|^2 - \lambda \text{Re}(\bar{\psi}_1 \psi_2) \right]. \quad (5)$$

The coupling term by itself is minimized with a solution such that $\arg \psi_1 = \arg \psi_2$. The analogy with the off-axis rotation of a single condensate [see Eq. (4)] suggests the variational wave function

$$\psi_{1,2}(x, y) \propto e^{-(x \pm u)^2 / 2 - y^2 / 2} e^{\mp i v y}. \quad (6)$$

Substituting this ansatz into Eq. (5), one gets an effective energy

$$E \sim \frac{1}{2}(u-d)^2 + \frac{1}{2}v^2 + \Omega uv - \lambda e^{-u^2} + g_{12} C e^{-2u^2}, \quad (7)$$

where C is of order unity. Minimization with respect to the velocity v leads to $v = -\Omega u$, and thus Ω favors separation. More importantly, it is clear from Eq. (7) that λ effectively decreases the repulsion between condensates. Thus, the separation u decreases with the strength of the optical coupling and becomes zero for a strong enough value of the Josephson coupling, λ_c . Both the repulsive interaction among bosons and the rotation of the trap tend to inhibit mixture of species, thus increasing the value of λ_c . For high enough λ , the two components become essentially miscible.

IV. VORTEX FORMATION

The structure of matter flow in the condensate suffers a drastic transformation when the Josephson coupling is introduced. The numerical results for setups *A* and *B* show that, for some frequencies, the existence of a nonzero coupling permits the formation of vortices that would be otherwise forbidden [Figs. 3(a) and 4]. These vortices involve a matter flow which is orthogonal to the wall separating both condensates [Fig. 3(b)]. We note that the exact location of both vortex cores depends on the intensity of the coupling [Fig. 3(d)].

The mathematical reason for this striking change is that, with a nonzero value of λ , the matter flow of each species is no longer conserved. Assuming a divergence-free flow, the equation of continuity along the trajectory of a boson becomes

$$\frac{\partial |\psi_1|^2}{\partial l} v_1 = -\lambda \operatorname{Re}(\bar{\psi}_1 \psi_2) = -\frac{\partial |\psi_2|^2}{\partial l} v_2. \quad (8)$$

Thus, as the current line is closed around the origin, there is an exchange of bosons among components. A typical boson flowing around the origin suffers a transformation from state $|1\rangle$ to $|2\rangle$ and vice versa as it completes a circle.

Physically, there is a fundamental reason why bosons are transferred from one component to the other. For $\lambda = 0$, vortices must lay inside each condensed cloud, due to current

conservation, which means that a large angular speed is required to create them. However, for any nonzero coupling, vortices may appear *outside* the bulk of the clouds, at a variable distance from the origin. Placed at low-density regions, the twist of the phase requires less kinetic energy $\int |\psi_i|^2 (\nabla \arg \psi_i)^2$ and provides more angular momentum than the mere separation of clouds.

In Figs. 4(a) and 4(b), we plot the angular momentum per particle as a function of the Josephson coupling and the angular speed. The cliffs on the surface are due to the nucleation of successive vortices. The separation of these vortices from the $x=0$ domain wall decreases very fast with increasing λ : Fig. 3(d) shows that, already for $\lambda = 0.05$, the vortices become visible. The limit $\lambda \rightarrow 0^+$ for fixed Ω is physically smooth because in it vortices disappear continuously moving their core to infinity, and carry a vanishing mass flow, as evidenced in Fig. 4 by the decreasing height of the first step. At $\lambda = 0$, a much higher angular speed is needed to create vortices, because these are necessarily off-axis (here, $\Omega > 0.45$ is required). The main result is that a moderate optical coupling ($\lambda \sim 0.1$) permits the formation of split vortices with important mass flow at lower angular velocities.

V. INTERNAL JOSEPHSON DYNAMICS

The Hamiltonian (5) may be written as that of a nonrigid pendulum [8] with an effective interaction energy $E_c = \sum_{ij} g_{ij} \sigma_{ij} (-1)^{i+j}$, where $\sigma_{ij} \equiv \int |\psi_i|^2 |\psi_j|^2$, and an effective Rabi frequency $\omega_R = \Omega_R s_{12}$, with $s_{12} \equiv \int \bar{\psi}_1 \psi_2$. The conclusion is that, for the setups considered here ($\lambda \leq 0.5$), the internal two-state dynamics lies in the collective Josephson regime ($2\omega_R/N \ll E_c \ll N\omega_R/2$), while in the JILA experiment [6], where no walls are formed, the same dynamics lies in the noninteracting Rabi limit ($E_c \ll 2\omega_R/N$).

ACKNOWLEDGMENT

This work has been partially supported by the Ministerio de Ciencia y Tecnología under Grant Nos. BFM2000-0521 and PB96-0080-C02.

-
- [1] M.R. Matthews, B.P. Anderson, P.C. Haljan, D.S. Hall, C.E. Wieman, and E.A. Cornell, *Phys. Rev. Lett.* **83**, 2498 (1999).
 [2] K.W. Madison, F. Chevy, W. Wohlleben, and J. Dalibard, *Phys. Rev. Lett.* **84**, 806 (2000); F. Chevy, K.W. Madison, and J. Dalibard, *ibid.* **85**, 2223 (2000); J.R. Abo-Shaeer, C. Raman, J.M. Vogels, and W. Ketterle, *Science* **292**, 476 (2001).
 [3] See, e.g., A. Svidzinsky and A.L. Fetter, *J. Phys. B* **13**, R135 (2001), F. Sols, *Physica C* **369**, 125 (2002); and references therein.
 [4] D.L. Feder *et al.*, *Phys. Rev. Lett.* **86**, 564 (2001); F. Dalfovo and S. Stringari, *Phys. Rev. A* **63**, 011601 (2001).
 [5] J.J. García-Ripoll and V.M. Pérez-García, *Phys. Rev. A* **64**, 013602 (2001).
 [6] D.S. Hall, M.R. Matthews, C.E. Wieman, and E.A. Cornell, *Phys. Rev. Lett.* **81**, 1543 (1998).
 [7] B.P. Anderson and M.A. Kasevich, *Science* **282**, 1686 (1998).
 [8] For a review, see F. Sols, in *Proceedings of the International School of Physics "Enrico Fermi,"* edited by M. Inguscio *et al.* (IOS Press, Amsterdam, 1999), p. 453.
 [9] B.D. Esry and C.H. Greene, *Nature (London)* **392**, 434 (1998).
 [10] S. Coen and M. Haelterman, *Phys. Rev. Lett.* **87**, 140401 (2001).
 [11] D.S. Hall, M.R. Matthews, J.R. Ensher, C.E. Wieman, and E.A. Cornell, *Phys. Rev. Lett.* **81**, 1539 (1998).
 [12] A. Görlitz *et al.*, *Phys. Rev. Lett.* **87**, 130402 (2001).
 [13] J.J. García-Ripoll, V.M. Pérez-García, and V. Vekslerchik, *Phys. Rev. E* **64**, 056602 (2001).